Modeling of Water Contents in Concrete Using Electromagnetic Guided Waves

*XIAO Xiaoting**[1], IHAMOUTEN Amine[2], VILLAIN Géraldine[3], DEROBERT Xavier[3], TIAN Guiyun[1]*

[1]College of Automation Engineering, University of Electronic Science and Technology of China, Chengdu 611731, China

[2]Cerema, Les Ponts-de-Cé 49136, France

[3]Ifsttar, Route de Bouaye, CS4, Bouguenais F-44344, France

Abstract: Concrete has been widely used as a building material for the last decades. As we know, the degradation of concrete happens mostly with the presence of water, to which the electromagnetic waves are sensitive. The information of water content in concrete structure thus becomes an interesting subject for ground penetrating radar (GPR). In this study, we use an experimental set-up of imbibition to model the water content in concrete. Our main objective is to monitor the water transfer through time by electromagnetic (EM) guided waves. A new empirical model – arctan(x) model is proposed here to approximate the distribution of dielectric constant in concrete slabs during imbibition time, based on the measurements of gammadensimetry. The determination procedure includes the requirement of guided waves, the extraction of phase velocity dispersion curves and the inversion of gradient curves. The inversion of this model has been validated first by synthetic model in Matlab®, then by numerical model using GPR modeling software GprMax 2D, where the concrete with gradient was approximated by a 27-layer medium. The model will be further validated by experimental studies. The GPR equipped with antennas at 1.5 GHz will be applied to the measurements of guided waves using common mid-point (CMP) configuration. It can help us to design and develop new microwave (MW) sensing and imaging systems for structural health monitoring of multiple layers of concrete.

Key words: Ground penetrating radar, Common mid-point, Concrete, Water content, Guided waves

CLC number: **Document code:** **Article ID:**

0 Introduction

Concrete, especially reinforced concrete, is certainly the most popular building material today [1]. For the last decades, it has been widely used in the constructions of housing, factories, commercial buildings, bridges, tunnels and other infrastructures. The durability of concrete thus becomes a main issue to concern as there always exists degradation of concrete. One of the main degradation processes is the steel corrosion, causing cracks in concrete cover and weakening the strength of concrete structures [2-4]. This process is caused by the penetration of aggressive agents, which is associated with the penetration of water. As we know, water content of concretes is an import durability monitoring parameter, which causes and accelerates most degradation processes.

There are a lot of non-destructive testing (NDT) methods that can be applied to the detection of concrete, such as resistivity [4], ultrasonic tests [5], thermographic imaging [6], and electromagnetic (EM) methods, including EM emission [7], ground penetrating radar (GPR) [8-9], etc. Among them, GPR is a competitive means for the detection of water content as the measurement is simple and the EM waves are sensitive to the presence of water. In fact, many studies have been announced about the determination of water content using GPR, according to the amplitudes, waveforms or propagation velocities of GPR pulses [10-11].

However, in these studies, the concrete specimens are usually considered as homogeneous media. It is not applicable to most in-situ measurements as there are water gradients in concrete structures in natural environment. As an important step to study the water transfer in concrete, we use an experimental set-up of imbibition to model the water content in concrete. The partially wet concrete slab, with the water or a steel sheet below, can form a waveguide (WG) for the propagation of EM waves. The study of van der Kruk [12] announced that it is possible to invert the physical properties of the WG medium from the dispersion of the guided GPR

***Corresponding author:** Xiao Xiaoting, Doctor, E-mail: xt_xiao@foxmail.com.

waves. The propagation of transverse electric (TE) modes is less sensitive to EM leakage phenomena, corresponding to the model we use. In our former works[13], we suppose the concrete slab as a two-layer medium, composed of a dry layer and a wet layer. The thickness of each layer has been successfully calculated from the WG inversion. However, the two-layer model is only available when there is a sharp interface between the dry part and the wet part. In most cases, a transition zone exists between the two parts [14], which can be observed as a water gradient. Then we found from the results of gammadensimetry [15] that, the water content gradient curve in concrete is like a reversed arctan curve. In this case, a new empirical model – arctan(x) model is proposed here to approximate the gradients in concrete slabs. The main objective is to better determine the water content in concrete during imbibition.

The rest of this paper is organized as follows: section 1 talks about the fundamental equations for WG inversion and the introduction of parallel model; section 2 introduces the experiment of concrete imbibition and the reference results obtained from gammadensimetry; section 3 discusses about the modeling of partially wet concrete slab during imbibition using arctan(x) model; section 4 presents the conclusions of this paper.

1 Inversion of EM WG Model

The theories related to the multi-layer WG inversion are to be introduced in this section. The fundamental equation of the modal theory is used to calculate the theoretical phase velocities at different propagation modes, with the knowledge of incident angle. The parallel model is a dielectric mixing model which can develop the one-layer waveguide into multi layers. This section lays the foundation of the inversion for the arctan(x) model.

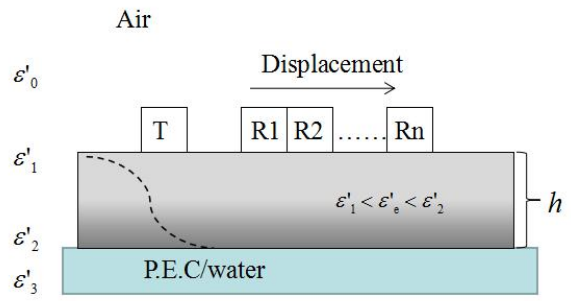

Fig.1 Diagram of GPR monitoring with a WARR-TE configuration for EM wave propagation in a leaky WG

1.1 Fundamental equations

As shown in Fig.1, a concrete slab forms a leaky WG[8] for the propagation of GPR waves, with a perfect electric conductor (PEC) or some water below.

A dielectric mixing model - parallel model is used to define the real part of the equivalent permittivity ε'_e of the WG medium. Note that the WG is low loss medium and the value of ε'_e is between the dielectric constant of the two ends: $\varepsilon'_1 < \varepsilon'_e < \varepsilon'_2$. The fundamental equation of modal theory can thus be defined by:

$$1 - R_{e3}^{TE}(\theta) R_{e0}^{TE}(\theta) \exp\left[-2j\sqrt{\varepsilon'_e}\frac{\omega}{c_0} h\cos(\theta)\right] = 0 \quad (1)$$

where $j = \sqrt{-1}, c_0 = 3\times10^8 m/s$, ω is the angular frequency, θ is the incident angle, h is the total thickness of the waveguide, R_{e0}^{TE} and R_{e3}^{TE} are the reflection coefficients of the transverse electric (TE) modes at the upper and lower boundaries of the WG, respectively.

The phase velocity v_φ is frequency dependent and determined by the following equation:

$$v_\varphi(f) = \frac{c_0}{\sqrt{\varepsilon'_e}\sin\theta(f)} \quad (2)$$

The measured phase velocity v_φ^m is picked from a dispersion image calculated from the GPR data by a two dimensional Fourier transform [16]. The dielectric and geometric properties of the WG can be approximated by minimizing the difference between the measured and theoretical dispersion curves of phase velocity. The cost function is therefore given by:

$$CF(\varepsilon'_e, h) = \sum_{n=1}^{N} \frac{\left| v_\varphi\left(\theta\left(f_n, \varepsilon'_e, h\right)\right) - v_\varphi^m \right|}{N} \quad (3)$$

where N is the number of frequency points.

1.2 Parallel model

The parallel model [17], derived from Lichtenecker - Rother equation, is found to implement the gradients in the WG. The equivalent permittivity ε'_e is calculated from the permittivity and thickness of each layer ε'_i and h_i through the equation of parallel model:

$$\varepsilon'_e = \sum_{i=1}^{n} h_i \varepsilon'_i \Big/ \sum_{i=1}^{n} h_i \quad (4)$$

This model applies to the case that the interfaces among these media are regarded as parallel and infinite.

2 Imbibition of Concrete

An experiment of imbibition was undertaken for concrete by capillary effects with the application of two measurements: GPR and gammadensimetry. The concrete samples were strictly controlled in temperature and moisture conditions in a climate chamber before the experiment. The GPR was applied for the acquisition of guided waves. The measurements of gammadensimetry show the gradient curves of relative density of the concrete sample during imbibition, which can be considered as reference. However, as cylindrical samples are required for the measurements of gammadensimetry, it is usually classified as a semi-destructive test.

2.1 Experimental set-up

In the experiment of imbibition, a non-reinforced concrete slab with the size 45×36×13 cm^3 was first put in a climate chamber conditioning at T = 20 ℃ and relative humidity RH = 70% for two months to make the moisture distribution homogeneous. Then it was placed in a basin where the water surface is kept 2cm higher than the bottom of the concrete. The resin painted on the 4 sides of the slab ensures the water goes up into the concrete by capillary effect. At the same time, a cylindrical sample (size: Ø10 × 12 cm^2) of the same concrete is conditioned with the same protocol for the measurement of gammadensimetry. The experimental set-up of imbibition is demonstrated in Fig.2.

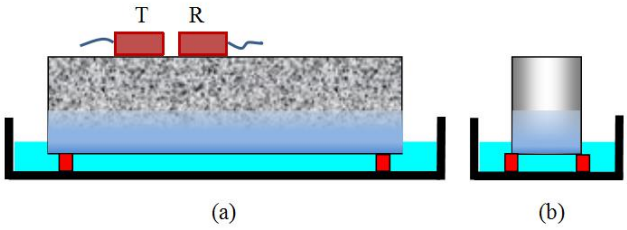

Fig.2 Imbibition protocol of: (a) concrete slab (45×36×13 cm^3) intended for GPR measurements; and (b) concrete cylindrical core (Ø10×12 cm^2) intended for weighing and gammadensimetry measurements

The concrete specimens were measured before putting into the water. Then the measurements were conducted after each certain time of imbibition. For the requirement of GPR data, the GPR system SIR-3000 from GSSI® equipped with 1.5 GHz antennas was used for a common mid-point (CMP) TE measurement. The offset between the transmitter and the receiver started from the middle to the maximum offset X_{max} = 28 cm, with a moving step Δx = 1 cm.

2.2 Gammadensimetry

Gammadensimetry [15] is a non-destructive equipment that generates γ-ray to measure the density and density variation over time of civil engineering materials.

The concrete core was measured at different height by every 6 mm to obtain the density variation curve. The results are shown in Fig.3, where t0 refers to the time before imbibition. The concrete sample was measured at the imbibition time of 2 h, 4 h, 8 h, 30 h and 124 h. During the first 30 hours of imbibition time, the density at the bottom and the top keeps at almost the same level. Despite some noise caused by the heterogeneity of concrete, the variation curves are like reversed arctan functions. However, after 124 hours, the concrete sample is nearly saturated. The curve is not like arctan function anymore.

The increase of water content is linearly related to the increase of density. Moreover, the water content has a strong linear relationship with the dielectric constant of concrete [18-19]. The gradient curve of dielectric constant in concrete is thus supposed to have the same shape as the density variation curve.

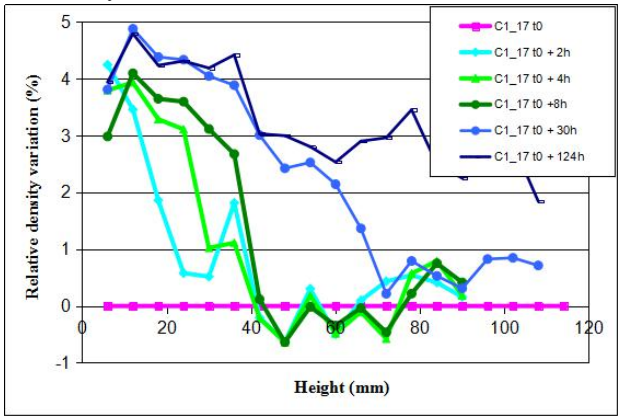

Fig.3 Relative density variation of cylindrical sample C1- 17 as function of height through imbibition time obtained by gammadensimetry

3 Simulation with Arctan(x) Model

Based on the results of gammadensimetry, an arctan(x) model is proposed here to present the variation of dielectric constant with respect to the position x of concrete's height h during imbibition:

$$\varepsilon'(x)=\frac{b-c}{\pi}\arctan\left(\frac{2d}{a}-\frac{2x}{a}\right)+\frac{b+c}{2} \quad (5)$$

In Eq. (5), $x\in[0,h]$, b and c are respectively the upper limit and lower limit of the curve, d refers to the position of the gradient and a is the shape factor that when $a\to 0$, the medium can be regarded as two layers and d is the thickness of the wet layer. The effective permittivity of the medium is given by the following equation, with applying the parallel model:

$$\varepsilon'_e=\frac{\int_0^h \varepsilon'(x)\mathrm{d}x}{h} \quad (6)$$

Since h is normally a known parameter, our objective becomes to invert the 4 parameters [*a, b, c, d*] by minimizing the cost function:

$$CF(a,b,c,d)=\sum_{n=1}^{N}\frac{\left|v_\varphi\left(\theta\left(f_n,a,b,c,d\right)\right)-v_\varphi^m\right|}{N} \quad (7)$$

The non-linear least squared algorithm is used to do the minimization. The proposed arctan(x) model will be verified by the numerical model simulated with the GPR modeling software gprMax 2D [20]. Then the inversion will be validated with the data from numerical model.

3.1 Gradient models

To build the synthetic model, the parameters of arctan(x) model are determined as: h = 0.13, a = 0.01, b = 15, c = 6 and d = 0.02. In gprMax, the variation of permittivity is approximated by a 27-layer medium. The conductivity is defined as σ = 0.00004 S/m so the medium can be considered as lossless. No dispersion is added to the material because the geometrical dispersion from the multi-reflections in the waveguide is only considered in our model. The WARR configuration is used in the GPR simulation. The resource is a ricker pulse at 1 GHz as it is similar to the emitted signal from the GPR system we use at 1.5 GHz. The offset between the transmitter and the receiver started from $X_{\min}$ = 9.4 cm to the maximum offset $X_{\max}$ = 39.4 cm, with a moving step Δx = 1 cm.

Fig.4 demonstrates the difference of dielectric constants from the analytical model and the numerical model for gprMax. It is shown that the permittivity of the model in gprMax (black line) is not exactly the same as the analytical model (purple line). The black line is getting closer to the purple line when the number of layers increases. However, considering the calculation efficiency, we only defined 27 layers.

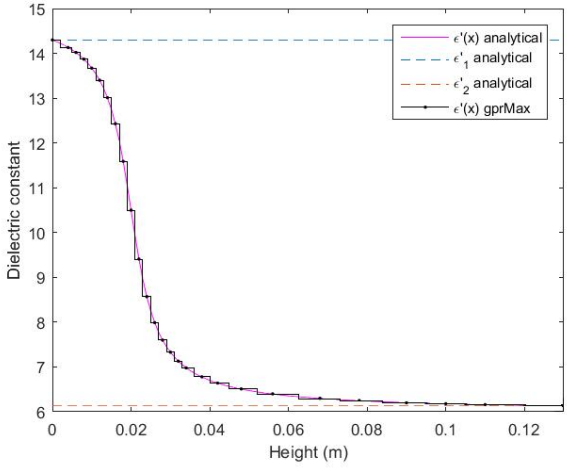

Fig.4 Gradient curves of permittivity from synthetic and numerical (gprMax) models

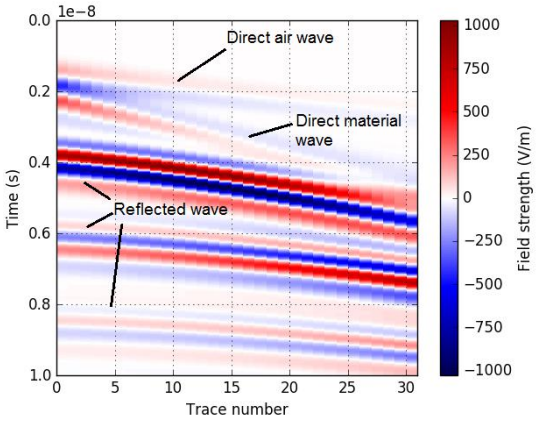

Fig.5 B-scan obtained from the WARR GPR simulation

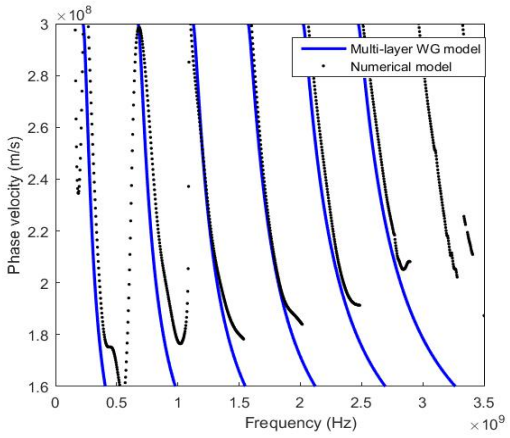

Fig.6 Dispersion curves of guided waves from synthetic arctan(x) model (blue line) and numerical model (black dot) with h = 0.13, a = 0.01, b = 15, c = 6 and d = 0.02

Fig.5 is the B-scan obtained from the GPR simulation which shows the multi-offset wave-field with respect to the trace number (refers to the offset) and the propagation time. From the figure, we can see very strong reflections in the waveguide medium. Then the whole wave-field was transformed into the $f-\beta$ [13] domain to pick the phase velocity dispersion curves.

Fig.6 shows the dispersion curves of the gradient model, calculated from the WG model and the numerical model, respectively. From the figure, we observe that the curves generally match well with each other. The errors at low frequencies are caused by the low resolution of $f-\beta$ [16] transform and the limitation of $X_{\max}$. The errors at high frequencies are probably caused by the multi-reflections among the different layers as waves at higher frequency are more sensitive to the variation of permittivity. In this case, values at low frequencies and high frequencies, normally below 500 MHz and above 2.5 GHz for the 1.5 GHz antennas, are not preferred in the inversion since they will introduce more errors into the inversion results. In the following subsection, the dispersion curves from the numerical model will be used to validate the inversion of the WG model. Some details will also be discussed in the process.

3.2 Validation of WG inversions

By integrating the arctan function equations (5) and (6) into the WG model, our inversion is targeted at the estimation of the parameters [*a, b, c, d*]. Two steps have been conducted for the validation: first, to study the cost function with the analytical model; second, to validate the inversion with the numerical model. Then the arctan(*x*) model will be applied to the experiments on concrete of imbibition.

To look for the global minimum of the cost function min(*CF*), we have calculated the values of *CF* by varying 3 out of the 4 parameters. It has been proved that one global minimum can be found if we properly define the initial values of the 3 unknowns. However, there are also many local minima. We can imagine that the inversion of the 4 unknowns would be much more difficult. After some parametric study on the 4 parameters, we finally decided to pre-estimate parameter *c* and to invert the other 3 parameters since *CF* is less sensitive to the error in *c* and *c* refers to the value of ε'_1, which is possible to be obtained in reality. The steps of inversion are described as follows.

1) Selection of working band. The first step of the inversion is to select the frequency band to be used for the phase velocities. The modes TE_1 (0.7 – 0.9 GHz), TE_2 (1.2 – 1.4 GHz) and TE_3 (1.7 - 1.9 GHz) are finally chosen to do the calculation.

2) Initial values of iterations. The initial values of the iterations are determined in Table 1. The parameter *b* is close to the dielectric constants of the lower surface of the waveguide. For concrete slabs, we are able to limit its value in a certain range by experience. The shape factor *a* is normally located between 0.01 and 0.04. The value of *d* corresponds to the position of the water front, which we can determine it between 0 and the total thickness *h*. But here we use the range [0.01 - 0.06] (m) to save the time.

Table 1 Definition of starting values of inversion

Parameter	Range	Interval
a	0.01 – 0.04	0.01
b	12 – 18	1
d	0.01 – 0.06	0.01

3) Minimum *CF* searching. For each combination of the starting values of the 3 parameters, one min(*CF*) is obtained in the end, which is the residue of the non-linear regression. The minimum of the cost functions min(*CF*) from all the starting models is identified as the global minimum or very close to it, where we get the values of [*a,* b, d] that we are looking for.

The inversion has been done for the analytical WG model and the numerical model built in gprMax. The results are shown in Table 2, where the direct values refer to the input values for the arctan(*x*) gradient model. The calculations have been proceeded with one single mode, as well as two combined modes. For the results of the analytical WG model, the inverted parameters match very well with the input parameters. Furthermore, the residue is rather small. For the results of the numerical model, it is not so good as the WG model. The approximation of ε'_1 is good because parameter *c* is considered as a known parameter. However, from the inversion results of TE_1 mode, the values of *b* and *d* are obviously smaller than the model, resulting the error in ε'_2. This is reasonable because the phase velocities of the numerical model at TE_1 are obviously higher than those of the WG model, as we can find in Fig.6. When we combine TE_1

and TE_2 modes, the inversion results seem to be better. Meanwhile, we find the inversion results from TE_2 and TE_3 modes are rather satisfying as the dispersion curves match very well with the WG model. Comparing the inversion results of the two models, we can conclude that the 3 parameters [*a, b, d*] of arctan(*x*) model can be inverted directly from the phase velocities of the guided waves. The selection of frequency band is essential since the errors in dispersion curves will cause errors in inversion results. When multiple modes are involved in the inversion, the errors can be reduced.

4 Conclusion and Future Works

In this paper, we have proposed an empirical model – arctan(*x*) model to describe the gradient curve of partially wet concrete slabs during imbibition. It has been built according to the reference results from gammadensimetry. By combing this model with the parallel model, we find it possible to invert the gradient curve of permittivity from the propagation velocities of guided waves. It can be applied to the concrete of imbibition when the slabs are un-saturated. To correctly invert the unknown parameters, the working frequency band should be carefully chosen. The accuracy of inversion results will also be affected by the accuracy of dispersion curves. To obtain a complete wave-field of the guided waves, it is important to note the criteria to form the WG. A strong reflector, such as a metal sheet, is often acquired below the WG medium.

In the next step, we will apply this model to the experimental results for validation. We also hope to validate the process to a more general case, for example, to design and develop new microwave (MW) sensing and imaging systems for structural health monitoring of multiple layers of concrete. The challenge may be that, for multiple layers, the current model will not be available. More unknowns will be in the inversion, bringing about more uncertainties to the solution. Considering the GPR measurements, the accuracy is also expected to be developed by reducing the noise and properly setting the experimental configurations.

Acknowledgment

The authors would like to thank the "Pays de la Loire" Regional Council for their financial support to the project.

Table 2 Inversion results of gradient models

Mode	*a*	*b*	*d*	ε'_2	ε'_1	min(*CF*) (10^6 m/s)
Direct values	0.01	15	0.02	14.3	6.13	
TE_1 – analytical	0.01	14.99	0.02	14.29	6.13	0.061
TE_2 – analytical	0.01	14.99	0.02	14.29	6.13	0.066
TE_3 – analytical	0.01	14.99	0.02	14.29	6.13	0.066
TE_1 – numerical	0.02	13.22	0.01	11.48	6.16	5.44
TE_2 – numerical	0.01	14.14	0.02	13.54	6.12	2.84
TE_3 – numerical	0.01	14.50	0.02	13.85	6.12	0.85
TE_1+TE_2 - numerical	0.02	15	0.01	12.75	6.24	4.47
TE_2+TE_3 - numerical	0.01	14.40	0.02	13.73	6.12	3.00

References:

[1] Mehta P K. CONCRETE: Microstructure, Properties, and Materials [M]. 3rd Edition. McGraw-Hill, 2006.

[2] Li J, Wu J. Analysis of reinforcement corrosion in reinforced concrete structures [J]. Journal of Nanjing University of Aeronautics & Astronautics, 2012, 44(4): 592 - 596.

[3] Zhang H, Yang R Z, He Y Z, et al. Identification and characterisation of steel corrosion using passive high

frequency RFID sensors [J]. Measurement, 2016: 421 - 427.

[4] du Plooy R, Villain G, Palma L S, et al. Electromagnetic non-destructive evaluation techniques for the monitoring of water and chloride ingress into concrete: a comparative study [J]. Materials and Structures, 2015, 48(1-2): 369 – 386.

[5] Garnier V, Piwakowski B, Abraham O, et al. Acoustic techniques for concrete evaluation: Improvements, comparisons and consistency [J]. Construction and Building Materials, 2013, 43: 598 – 613.

[6] Phillipson M C, Baker P H, Davies M, et al. Moisture measurement in building materials: an overview of current methods and new approaches [J]. Building Service Engineering Research and Technology, 2007, 28(4): 303 – 316.

[7] Han J, Huang S L, Wang S, et al. Coupled stress-electricity model for electromagnetic emission [J]. Transactions of Nanjing University of Aeronautics & Astronautics, 2015, 32(3): 334 - 340.

[8] Gao B, Woo W L, Tian G Y, et al. Unsupervised diagnostic and monitoring of defects using waveguide imaging with adaptive sparse representation [J]. IEEE Transactions on Industrial Informatics, 2015, 12(1):405-416.

[9] Lai W L, Tsang W F. Characterization of pore systems of air/water-cured concrete using ground penetrating radar (GPR) through continuous water injection [J]. Construction and Building Materials, 2008, 22(3): 250 – 256.

[10] Klysz G, Balayssac J P. Determination of volumetric water content of concrete using ground-penetrating radar [J]. Cement and Concrete Research, 2007, 37(8): 1164 – 1171.

[11] Kalogeropoulos A, van der Kruk J, Hugenschmidt J. Monitoring the evolution of water and chloride in concrete using GPR full-waveform inversion [C]. Proceeding of 6th International Workshop on Advanced Ground Penetrating Radar (IWAGPR), June 22-24, 2011.

[12] van der Kruk J, Arcone S A. Fundamental and Higher Mode Inversion of Dispersed GPR Waves Propagating in an Ice Layer [J]. IEEE Transactions on Geoscience and Remote Sensing, 2007, 45(8): 2483 – 2491.

[13] Xiao X, Ihamouten A, Villain G, et al. Use of Electromagnetic Two-layer Wave-Guided Propagation in the GPR Frequency Range to Characterize Water Transfer in Concrete [J], NDT & E International, available online 24 August 2016.

[14] Louis A, Van Der Wielen A, Courard L, et al. GPR detection of saturated areas into concrete in the presence of a water gradient [C]. Proceeding of 14th International Conference on Ground Penetrating Radar (GPR), June 4-8, 2012.

[15] Villain G, Thiery M. Gammadensimetry: A method to determine drying and carbonation profiles in concrete [J]. NDT & E International, 2006, 39(4): 328 – 337.

[16] Ihamouten A, Villain G, Dérobert X. Complex permittivity frequency variations from multioffset gpr data: Hydraulic concrete characterization [J]. IEEE Transactions on Instrumentation and Measurement, 2012, 61(6): 1636 – 1648.

[17] Wu Y, Zhao X, Li F, et al. Evaluation of mixing rules for dielectric constants of composite dielectrics by mc-fem calculation on 3d cubic lattice [J]. Journal of Electroceramics, 2003, 11(3):227 – 239.

[18] Soutsos M, Bungey J, Millard S. Dielectric properties of concrete and their influence on radar testing [J]. NDT & E international, 2001, 34: 419 – 425.

[19] Viriyametanont K, Laurens S, Klysz G, et al. Radar survey of concrete elements: Effect of concrete properties on propagation velocity and time zero [J]. NDT & E International, 2008, 41(3): 198 – 207.

[20] Giannopoulos A. Modelling ground penetrating radar by GprMax [J]. Construction and Building Materials, 2005, 19(10): 755 – 762.